

Lawrence Berkeley National Laboratory

Recent Work

Title

90-MEV NEUTRON-PROTON SCATTERING AT LARGE PROTON ANGLES

Permalink

<https://escholarship.org/uc/item/5z05j66b>

Author

Wallace, Roger

Publication Date

1950-09-05

UCRL 869

cy 2.

UNIVERSITY OF
CALIFORNIA

*Radiation
Laboratory*

TWO-WEEK LOAN COPY

*This is a Library Circulating Copy
which may be borrowed for two weeks.
For a personal retention copy, call
Tech. Info. Division, Ext. 5545*

BERKELEY, CALIFORNIA

DISCLAIMER

This document was prepared as an account of work sponsored by the United States Government. While this document is believed to contain correct information, neither the United States Government nor any agency thereof, nor the Regents of the University of California, nor any of their employees, makes any warranty, express or implied, or assumes any legal responsibility for the accuracy, completeness, or usefulness of any information, apparatus, product, or process disclosed, or represents that its use would not infringe privately owned rights. Reference herein to any specific commercial product, process, or service by its trade name, trademark, manufacturer, or otherwise, does not necessarily constitute or imply its endorsement, recommendation, or favoring by the United States Government or any agency thereof, or the Regents of the University of California. The views and opinions of authors expressed herein do not necessarily state or reflect those of the United States Government or any agency thereof or the Regents of the University of California.

UNIVERSITY OF CALIFORNIA
Radiation Laboratory

Contract No. W-7405-eng-48

UNCLASSIFIED

90 Mev Neutron-Proton Scattering at Large Proton Angles

Roger Wallace

September 5, 1950

Berkeley, California

INSTALLATION:

No. of Copies

Argonne National Laboratory	8
Armed Forces Special Weapons Project	1
Atomic Energy Commission, Washington	2
Battelle Memorial Institute	1
Brush Beryllium Company	1
Brookhaven National Laboratory	4
Bureau of Medicine and Surgery	1
Bureau of Ships	1
Carbide and Carbon Chemicals Division (K-25 Plant)	4
Carbide and Carbon Chemicals Division (Y-12 Plant)	4
Chicago Operations Office	1
Columbia University (J. R. Dunning)	1
Columbia University (G. Failla)	1
Dow Chemical Company	1
H. K. Ferguson Company	1
General Electric, Richland	3
Harshaw Chemical Corporation	1
Idaho Operations Office	1
Iowa State College	2
Kansas City Operations Branch	1
Kellex Corporation	2
Knolls Atomic Power Laboratory	4
Los Alamos Scientific Laboratory	3
Mallinckrodt Chemical Works	1
Massachusetts Institute of Technology (A. Gaudin)	1
Massachusetts Institute of Technology (A. R. Kaufmann)	1
Mound Laboratory	3
National Advisory Committee for Aeronautics	1
National Bureau of Standards	3
Naval Radiological Defense Laboratory	2
New Brunswick Laboratory	1
New York Operations Office	3
North American Aviation, Inc.	1
Oak Ridge National Laboratory	8
Patent Branch, Washington	1
Rand Corporation	1
Sandia Corporation	1
Santa Fe Operations Office	2
Sylvania Electric Products, Inc.	1
Technical Information Division (Oak Ridge)	15
USAF, Air Surgeon (Lt. Col. R. H. Blount)	1
USAF, Director of Armament (Captain C. I. Browne)	1
USAF, Director of Research and Development (Col. R. J. Mason, Fred W. Bruner)	2
USAF, Eglin Air Force Base (Major A. C. Field)	1
USAF, Kirtland Air Force Base (Col. Marcus F. Cooper)	1
USAF, Maxwell Air Force Base (Col. F. N. Moyers)	1
USAF, NEPA Office	2
USAF, Office of Atomic Energy (Col. H. C. Donnelly, A. A. Fickel)	2
USAF, Offutt Air Force Base (Col. H. R. Sullivan, Jr.)	1
USAF, Wright-Patterson Air Force Base (Rodney Nudenberg)	1

INSTALLATION:	No. of Copies
U. S. Army, Atomic Energy Branch (Lt. Col. A. W. Betts)	1
U. S. Army, Army Field Forces (Captain James Kerr)	1
U. S. Army, Commanding General, Chemical Corps Technical Command (Col. John A. MacLaughlin thru Mrs. Georgia S. Benjamin)	1
U. S. Army, Chief of Ordnance (Lt. Col. A. R. Del Campo)	1
U. S. Army, Commanding Officer, Watertown Arsenal (Col. C. H. Deitrick)	1
U. S. Army, Director of Operations Research (Dr. Ellis Johnson)	1
U. S. Army, Office of Engineers (Allen O'Leary)	1
U. S. Army, Office of the Chief Signal Officer (Curtis T. Clayton thru Maj. George C. Hunt)	1
U. S. Army, Office of the Surgeon General (Col. W. S. Stone)	1
U. S. Geological Survey (T. B. Nolan)	2
USAF, Director of Plans and Operations (Col. R. L. Applegate)	1
U. S. Public Health Service	1
University of California at Los Angeles	1
University of California Radiation Laboratory	5
University of Rochester	2
University of Washington	1
Western Reserve University	2
Westinghouse Electric Company	4
Naval Medical Research Institute	1
California Institute of Technology (R. F. Bacher)	1
TOTAL	138

Information Division
 Radiation Laboratory
 University of California
 Berkeley, California

90 Mev Neutron-Proton Scattering at Large Proton Angles

Roger Wallace

Radiation Laboratory, Department of Physics
University of California, Berkeley, California

September 5, 1950

Abstract

Neutron-proton scattering with 90 Mev neutrons has been investigated by others,^{1,2} using a proportional counter technique and also using a cloud chamber. They measured the scattering cross section for neutrons for center of mass angles from 36° to 180° . The present experiment was an attempt to overlap the data of Hadley, et al.¹ from 74° to 36° and to extend the cross section measurements to smaller angles. This experiment was performed with nuclear emulsions in order to permit the detection of protons down to about 1.5 Mev, and to avoid systematic errors that might be present in the case of other methods of detection. The results agree with those of Hadley, et al., within the probable error, and the cross section curve exhibits beyond 36° the same general trend as the curve measured by Hadley, et al. The measurements confirm the fact that there is probably not complete symmetry of the n-p cross section curve about 90° in the center of mass system.

¹ J. Hadley, E. L. Kelly, C. E. Leith, E. Segre, C. Wiegand, and H. York, Experiments on N-P Scattering with 90 and 40 Mev Neutrons, Phys. Rev. 75, 351 (1949)

² K. Brueckner, W. Hartsough, E. Hayward and W. Powell, Neutron-Proton Scattering at 90 Mev, Phys. Rev. 75, 555 (1949)

90 Mev Neutron-Proton Scattering at Large Proton Angles

Roger Wallace

Radiation Laboratory, Department of Physics
University of California, Berkeley, California

September 5, 1950

Introduction

Neutron-proton scattering cross sections have been measured using the 90 Mev neutrons from the 184-inch Berkeley cyclotron by several different investigators. Hadley, et al.,¹ used two different arrangements of proportional counters. Their results are shown in Figure 8. It is seen that their points do not lie on a curve that is symmetrical about 90° . This experiment was performed to find out if the cross section does rise in the small angle region. It has been felt by some that the cross section curve (Figure 8) was flat to the left of 70° and did not rise. The results of this experiment serve to confirm the rising slope of the curve in the small angle range, in agreement with Hadley, et al. Bruecker, et al.,² using a cloud chamber technique, have observed an angular dependence of the n-p cross section similar to that observed by Hadley, et al. The results of the present experiment also agree well with the cloud chamber data.

Apparatus and Procedure

The main part of the apparatus consisted of a nuclear plate camera, similar in design to that used by Panofsky and Fillmore.³ The camera and associated shielding (Figure 1) were mounted on a support, aligned in the 90 Mev neutron beam of the 184-inch cyclotron, similar to the paraffin

³ W. K. H. Panofsky and F. L. Fillmore, The Scattering of Protons by Protons near 30 Mev, Phys. Rev. 79, 57 (1950)

collimator mount used by Brueckner, et al.² The collimator was stopped down to a 1/2-inch diameter circle and additional lead bricks were added to reduce the background. The camera (Figure 2) differed from that used by Panofsky and Fillmore³ in that the plates were mounted farther from the beam and farther from each other. These dimensional changes were made since the neutron beam intensity of the cyclotron is much less than the proton beam intensity of the linear accelerator; thus, it was necessary to include more beam area with a consequent relaxation of the geometrical precision of the experiment. At each end of the camera-scattering chamber there was a 0.005-inch duraluminum foil window. The cyclotron beam, collimated to 1/2 inch, passed into and out of the camera through these foils. The exit foil was mounted on the end of a tube, as shown in Figure 2, in order to reduce the background on the plates that might have come from particles scattered from the exit foil. Particles that might have been scattered from the entrance foil entered the plates at such an angle that tracks caused by them, when viewed under a microscope, were easily distinguished from those coming from the hydrogen gas contained in the scattering chamber, since the desired tracks and the foil scattered tracks entered the field of view from different angular directions. Thus the particles scattered from the entrance foil constitute a non confusable background.

Four point screw supports permitted the paraffin collimator and the camera to be aligned coaxially within 1/16 inch. The alignment was carried out with an optical telescope and was checked by exposing, during the first few minutes of the cyclotron run, an x-ray film located in a known position on the camera. A 1/16-inch alignment tolerance does not introduce a first order source of error since the plates were arranged symmetrically around the beam and the angular distribution data from all plates were combined.

The plates were aligned in the camera by being held against a machined surface for which the geometric tolerance was less than 0.010 inch.

Two identical cameras were constructed, one for hydrogen exposures, the other for vacuum, background exposures. The exposures from which the data were taken were made for 405 minutes at an average of $27\frac{1}{2}$ R per hour, for the hydrogen run, and 65 minutes at an average of 28 R per hour, for the vacuum run. This made the hydrogen run 186 R and the neutron background run 30 R. The R is an arbitrary beam intensity unit approximately equal to 10^5 neutrons/cm² sec. which can be used to secure the ratio of the hydrogen to the vacuum exposure.

The first few trial runs with hydrogen in the camera resulted in completely blackened plates. At first it was thought that the blackening was caused by impurities in the hydrogen gas, so the hydrogen was passed through a hot palladium leak, thus separating all other elements with the possible exception of a minute trace of helium. Since the blackening still occurred with this purified hydrogen it was concluded that the hydrogen itself must attack the emulsion. Webb⁴ advised us later that it was possible the photographic emulsions were fogged by pure hydrogen gas. The reason that Panofsky and Fillmore³ did not experience this difficulty was that they used a lower hydrogen pressure than the two atmospheres used in this experiment, and somewhat shorter times during which the plates were exposed to the hydrogen. It was found that the blackening of the plates by the hydrogen was temperature sensitive, and that a reduction of temperature to -15° to -20° C would allow the plates to be only slightly fogged after 8 hours exposure. Consequently a jacket was installed around the camera intended for hydrogen exposure, which was filled with a eutectic mixture of rock salt and ice during the run.

⁴ Julian Webb, Eastman Kodak Company, private communication.

The plate temperature was thus maintained at about -15°C . Webb indicated that a reduction of the temperature to -15°C would probably not reduce the proton sensitivity of the plates.

The data (Table I, Column 2) were taken from the plates with a microscope operating at 570x scanning a swath 140 microns wide. The recoil proton tracks were identified by their specific ionization, their point of entrance, dive angles into the emulsion, their azimuth angle in the microscope field, and their range. When a track seen to start in the field of the microscope had been recognized as that of a proton, by its ionization density, the microscope was focused up and down to check the fact that the track dived into the emulsion at an angle that was compatible with the geometric location of the photographic plate relative to the neutron beam. If the track passed this test, the plate was moved until the point at which the track entered the emulsion was centered under the microscope reticule cross hairs. The cross hairs were then rotated until one was tangent to the track as near to the point of entry as possible. Panofsky and Fillmore³ explain how this may be done with a minimum of setting error. The azimuth angle of the entry point was then measured with a goniometer attached to one of the microscope eyepieces. This azimuth angle was the only datum recorded for each track.

The classical expression for the energy of the scattered protons varies as the cosine squared of the proton scattering angle. The incident neutron beam contains the distribution of energies given by Eq. (1), which will be discussed later. This distribution causes the protons that are scattered at any particular angle to also have an energy distribution. The energy distributions for proton recoil angles $\theta_L = 0^{\circ}$, 30° , and 45° in the laboratory system are shown in curves a, b, and c of Figure 3. Curves of this general

form give the emulsion range distributions and also the grain density distributions to be expected of the protons scattered at various angles.

Most spurious tracks were rejected on the basis of having the wrong ionization for their azimuth angle or because they were too short for their angle, although these rejection criteria did not need to be used on more than 2 percent of the otherwise acceptable tracks. Another reason for the rejection of tracks was that their dive angle into the emulsion was too steep for them to have been caused by protons coming from the beam cylinder. Tracks coming in the three other quadrants were easily eliminated, although their number was very limited. The scanning of vacuum background plates indicated that the confusable background was less than 2 percent.

Two observers examined 2734 tracks. Of these all proton recoils, 350 in number, observed in the 45° to 51° laboratory angle range were not included in the final results. These tracks were excluded since the specific ionization of tracks scattered at these angles, with energies of 35 to 50 Mev, is so low that an excessive number of tracks is missed by the observer. In addition 157 tracks in the angular range of 79° to 85° in the laboratory system were not included in the final results since, as will be mentioned later, the correction factor for tracks that do not reach the plates is too large. The two observers read the same plate areas for 200 tracks and found that each missed about 5 percent of the tracks. The tracks missed were evenly distributed over all angles from 45° to 85° so this is a minor source of error.

The plates used were Ilford, type C-2, with 50 micron emulsions. They were developed for 30 minutes at 68° F in developer consisting of one part of D19 mixed with six parts of water.

Treatment of Data

The uncorrected data are shown in Figure 4. The data are grouped into three degree intervals in the laboratory system, so any corrections in the angular measurement that are small compared to three degrees will not be noticeable. The relativistic correction (Figure 4, curve a) makes the observed laboratory scattering angle slightly smaller than the classical laboratory scattering angle.

The geometry of this experiment, although not nearly as precise as that of Panofsky and Fillmore,³ did not make important corrections necessary. The tracks were observed in swaths 1/40 microns wide as the slides were moved under the microscope in a direction parallel to the x coordinate (Figure 2). The swaths were all located within 1/2 inch of the edges of the plates nearest the beam. The position of the particular swath, in which the microscope was working, within the 1/2-inch wide band on the plates was not recorded as part of the data. It must be pointed out that there was no attempt made to determine from which part of the 1/2-inch diameter beam cylinder each individual track came, nor was any record kept of the point on the plates at which each particle struck the plates. Thus there is a random rectangular distribution of the probability of a particle landing on a plate with a particular value of y. In addition the probability of a particle coming from a particular part of the cylindrical, uniform intensity beam is a sine distribution in z. These two distributions introduce a geometric uncertainty which must be included in a consideration of the precision of the results. The two probability distributions, one in y and one in z must be combined by a folding process, which is really a two step random walk effect. Due consideration must be given to the geometrical relation between the angle θ observed in the microscope and the angle θ_L at which a particular proton is

actually scattered from the beam. The mean difference between these two angles shown by curve b in Figure 4 is seen to be less than $1/2^\circ$.

The upper limitation on the observable scattering angle θ is introduced by the limited range of the low energy, high angle, protons in the hydrogen gas. The range-energy relations for protons in hydrogen at 2 atmospheres and -15°C and in nuclear emulsions are shown in Figure 5. It was decided, on the basis of the experience of Panofsky and Fillmore,³ that emulsion tracks shorter than 30 microns should not be recorded. Tracks shorter than 30 microns are easy to miss in scanning the plates. When tracks shorter than 30 microns are found, it is difficult to make a good measurement of their emulsion entrance angle, and there are a larger number of short background tracks against which it is tedious to discriminate if one tries to measure proton tracks shorter than 30 microns.

Since it was the purpose of this experiment to extend the cross section curve to smaller angles it is important to investigate the limitations on the acceptability of the data in the small neutron angular range. There are four effects to be considered in deciding how far into the small angle region the data can be considered dependable. At about $\theta_L = 80^\circ$ the energy of the scattered protons becomes so small that all of them do not have a range in the hydrogen gas long enough to allow them to strike the plates. Also due to their low energy they experience appreciable amounts of small angle scattering in the hydrogen gas and in the photographic emulsions. This scattering introduces errors in the measurements of the scattering angles. Furthermore, in the region of 80° , as a result of the reduced proton energies as mentioned above, the ranges of the particles in the emulsions are in many cases too short to allow for accurate identification and measurement. The combined result of these four effects must be ascertained in order to evaluate

the data properly:

The neutron beam produced by the bombardment of a 1/2-inch beryllium target with 180 Mev deuterons is known to have a broad energy distribution. This distribution has been calculated by Serber,⁵ and measured by Hadley, et al.¹ For energies above the maximum of the distribution curve the calculated and measured results agree, but the measured results are higher than the theoretical ones for energies below the maximum. For the purposes of this experiment it was assumed that the probability $P(E)$ of an incident neutron having the energy E in Mev has the form:

$$P(E) = K \exp \left\{ - \left[\frac{(E-90)}{20} \right]^2 \right\} \quad (1)$$

This relation, (Figure 3, curve e), approximates the high energy distributions of both Serber⁵ and Hadley, et al., but only the measured values of Hadley, et al., for energies less than 90 Mev. It was further assumed that the neutron-proton scattering cross section is inversely proportional to the energy in the energy range considered. Thus the neutron distribution that is effective in producing recoil protons is given by:

$$P'(E)_0 = K (1/E) \exp \left\{ - \left[\frac{(E-90)}{20} \right]^2 \right\} \quad (2)$$

(Figure 3, curve a). The integral of this curve gives the fraction of the recoil protons coming from that part of the beam for which the energy is below any given value, (Figure 3, curve d). This relation will be used to calculate the fraction of the protons with energies too low to reach the plates at large scattering angles where the stopping power of the hydrogen is high. From the range-energy relations for protons, in hydrogen and emulsion (Figure 5) the energy of the protons entering the emulsion coming from different energy regions of the beam can be calculated as a function of

⁵ R. Serber, The Production of High Energy Neutrons by Stripping, Phys. Rev. 72, 1007 (1947)

the laboratory proton scattering angle, θ_L . From these energies the ranges in the emulsion for the protons from different beam energy intervals can be plotted as a function of the angle (Figure 6, curves a). Since no tracks shorter than 30 microns are to be considered, there will be a correction factor by which the track counts at various angles θ must be multiplied. The cutoff is shown crossing the three beam fraction curves. From the cutoff curve the initial correction curve is calculated (Figure 6, curve b). This correction does not include the effects of gas and emulsion scattering.

The combined probability distributions due to the small angle gas and emulsion scattering are shown in Figure 7, curves a. These are for particles that left the scattering centers at $\theta_L = 78^\circ$ and 79° . The probability distributions are multiplied point by point by the correction curve (Figure 6, b) and plotted on top of curves 7a, resulting in the peaks to the right of the maxima of the symmetric curves. The areas of these new curves as a function of the original scattering angle θ (Figure 7, curve b) are then the final correction factors. In reality the correction factor has a very small influence on the final cross section curve. The data that go into the single point for neutrons at 26° in the center of mass system are 71, 57, and 46 tracks at proton angles, $\theta_L = 76^\circ$, 77° , and 78° respectively. When the correction factor is applied the data are changed to 71, 62, and 62 respectively. This application of the cutoff correction factor raises the point at the center of mass angle of 26° by about 11 percent.

The corrected track counts, grouped in three degree intervals, as a function of proton laboratory angle (Table I, column 4) were converted to numbers proportional to the n-p scattering cross section as a function of the neutron center of mass angles by the relation:

$$(d\sigma/d\omega)_{cm} \propto N(\theta) \Delta\theta \left[(z^2 + y^2)/z \right] (1/\Delta (\cos \theta_{cm})) \quad (3)$$

where $N(\phi)_{\Delta\theta}$ is the data divided by true scattering angles θ instead of observed angles ϕ . Actually the difference between these angles (Figure 4, curve b) is such a slowly varying function of the angle that the correction for it was not applied. The geometrical factor $(z^2 + y^2)/z$ is independent of the scattering angle. As a result of the geometrical parameters, when the two 1/2-inch geometrical tolerances are combined properly, they produce a probable error of 1.54 inches in the geometrical factor, $(z^2 + y^2)/z$, whose mean value is 13.12 inches. This probable error only introduces a very small error into the relative cross section data which is combined with the statistical error and listed in Table I, column 7. The values of the $\Delta(\cos \theta)_{cm}$ factor of Eq. (3) for transformation from laboratory to center of mass angles are shown in Table I, column 5. The corrected data divided by these and multiplied by the factor 1.192×10^{-3} to normalize the results to the absolute cross sections of Hadley, et al.,¹ are given in Table I, column 6, and plotted with probable errors in Figure 8, in combination with the points measured by Hadley, et al.

Conclusions

The n-p scattering cross section can be measured with the nuclear emulsion method for 90 Mev neutrons between neutron angles in the center of mass system of approximately 26° to 80° . In general the results agree with those secured by Hadley, et al., with counters. The slopes of the curves agree between 36° and 60° . The results of this experiment confirm the increasing slope of the cross section curve in the small angle region; however the asymmetry of the curve about 90° is based on the Hadley data since the curve from this experiment is normalized to the Hadley results.

The author wishes to express his appreciation to Keith Brueckner who aided in the design of the apparatus, to Jack Steller who helped with the

runs and microscope reading, and to Professor W. K. H. Panofsky, under whose direction the work was carried out. This paper is based on work performed under the auspices of the Atomic Energy Commission.

Table I

1	2	3	4	5	6	7
Proton Laboratory Angle Range	No. of Tracks Observed	Mean Neutron C.M. Angle	No. of Tracks Corrected	$\Delta(\cos \theta)_{\text{cm}}$ Transformation Factor	$\left(\frac{d\sigma}{d\omega}\right)_{\text{cm}}$ in 10^{-27} cm^2 *	Combined Probable Error
46-48	114	86	114	0.06963		
49-51	181	80	181	0.06874		
52-54	241	74	241	0.06710	4.28	0.19
55-57	260	68	260	0.06472	4.80	0.20
58-60	280	62	280	0.06163	5.42	0.22
61-63	266	56	266	0.05787	5.48	0.22
64-66	270	50	270	0.05347	6.02	0.24
67-69	248	44	248	0.04848	6.11	0.26
70-72	240	38	240	0.04298	6.77	0.29
73-75	248	32	248	0.03699	8.01	0.34
76-78	174	26	195	0.03060	7.60	0.39
79-81	120	20				
82-84	32	14				
Total - 2734 Tracks Observed						

* Normalized to the cross sections of Hadley, et al., by the factor 1.192×10^{-3}

Figure Captions

Figure 1. Arrangement of the paraffin collimator and lead bricks in front of the scattering camera. The alternate cameras are shown. The vacuum camera is shown in bombardment position. The jacketed hydrogen chamber is shown at one side. The wood supports for the apparatus are not shown. Twelve nuclear track plates were arranged symmetrically around the beam at 30° intervals, of which one is indicated in the figure.

Figure 2. Geometrical location of the nuclear track plates relative to the neutron beam. The variables used in the measurements and calculations are shown. All variables are in the laboratory system. The relations between the scattering angle θ and the observed angle ϕ are indicated.

Figure 3. Functions dependent on the energy. Curves (a), (b), and (c) are the probability of a recoil proton being scattered at 0° , 30° , or 45° having a particular energy. It is seen that the absolute dispersion in energy decreases as the scattering angle increases. Curve (d) gives the percentage of the protons scattered at 0° with energy above a definite value E . This curve is secured directly from curve (e), the energy distribution of the "90 Mev" neutron beam from 184-inch Berkeley cyclotron.

Figure 4. Functions depending on the laboratory angle at which the protons recoil. Curve (a) gives the difference between the classical recoil angle and the relativistic recoil angle. This correction is seen to be small. Curve (b) shows the mean correction made necessary by the geometry. Curve (c) gives the mean path distance through the hydrogen gas in the scattering chamber from the points

of impact in the cylindrical beam region to the photographic plates. Curve (d) is a histogram of the raw data grouped in three-degree intervals. The data from 46° to 52° and from 79° to 82° was considered unreliable for reasons mentioned in the text. The data from 76° to 79° was corrected for limited proton range in the hydrogen and for small angle scattering in the gas and emulsion, as shown. Curve (e) is the multiplication factor for converting the laboratory coordinate data of curve (d) to the center of mass data of Figure 8. The conversion factor is calculated for the same three-degree intervals into which the data is divided.

Figure 5. Range-energy curves for protons in hydrogen gas at 2 atmospheres and -15° C and in nuclear track emulsion.

Figure 6. The experimental cutoff of tracks at the large proton angle limit is based on the three curves (a) of proton range in the emulsion for protons scattered at the angles shown, coming from the three positions on the beam energy distribution shown on curve (d),

Figure 3. The 30-micron cutoff shown above is explained in the text. Curve (b), the multiplicative correction factor that must be applied to the data as a result of the cutoff, is secured from the three curves (a) directly, and includes no correction for gas scattering.

Figure 7. The symmetrical parts of curves (a) are the superposition of the small angle gas and emulsion scattering probabilities for protons scattered at 78° and 79° in the laboratory system. Since some of these particles are viewed on the plates at angles greater than 79° and are thus partially not counted as a result of the cutoff

shown on Figure 6, a correction must be applied to the recorded data. The correction curve shown in Figure 6(b) has been multiplied by curves 7(a) point by point and the results are the asymmetrical bumps shown on the right side of each curve. The areas of the resulting curves are the correction factors that must be applied to the recorded data and these factors are given by curve (b).

Figure 8. The final corrected data are shown by the circles above. The results of Hadley, et al.,¹ are shown by the triangles. It is seen that the slopes of the results of the two experiments agree between 36° and 60° .

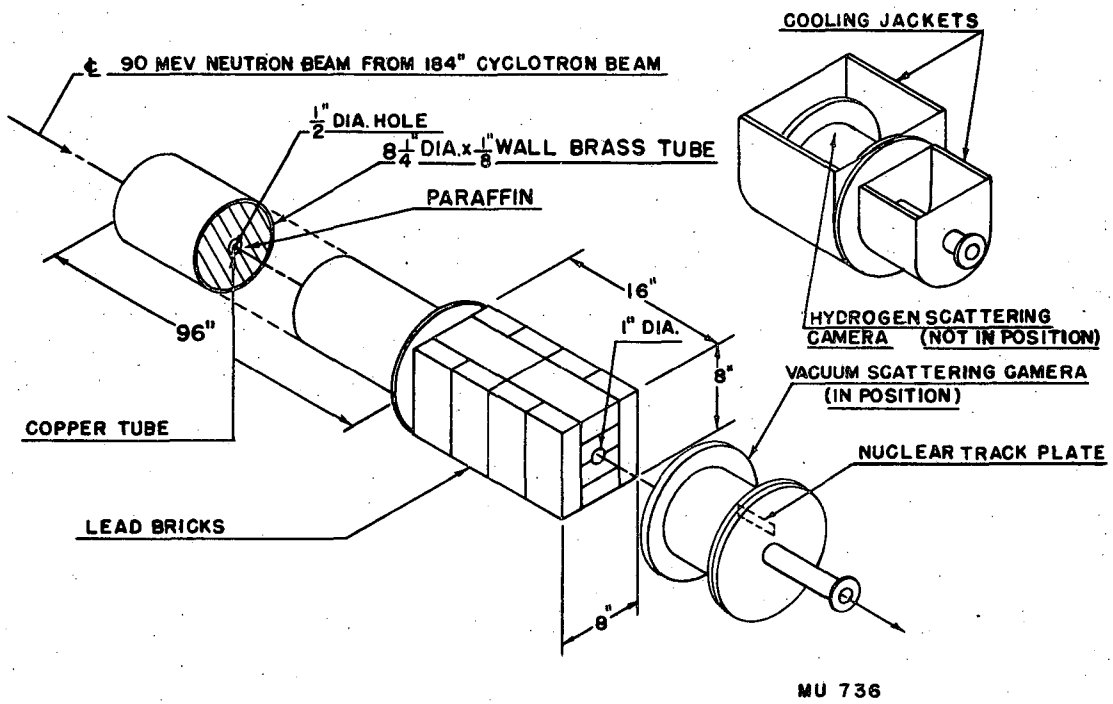


FIGURE 1

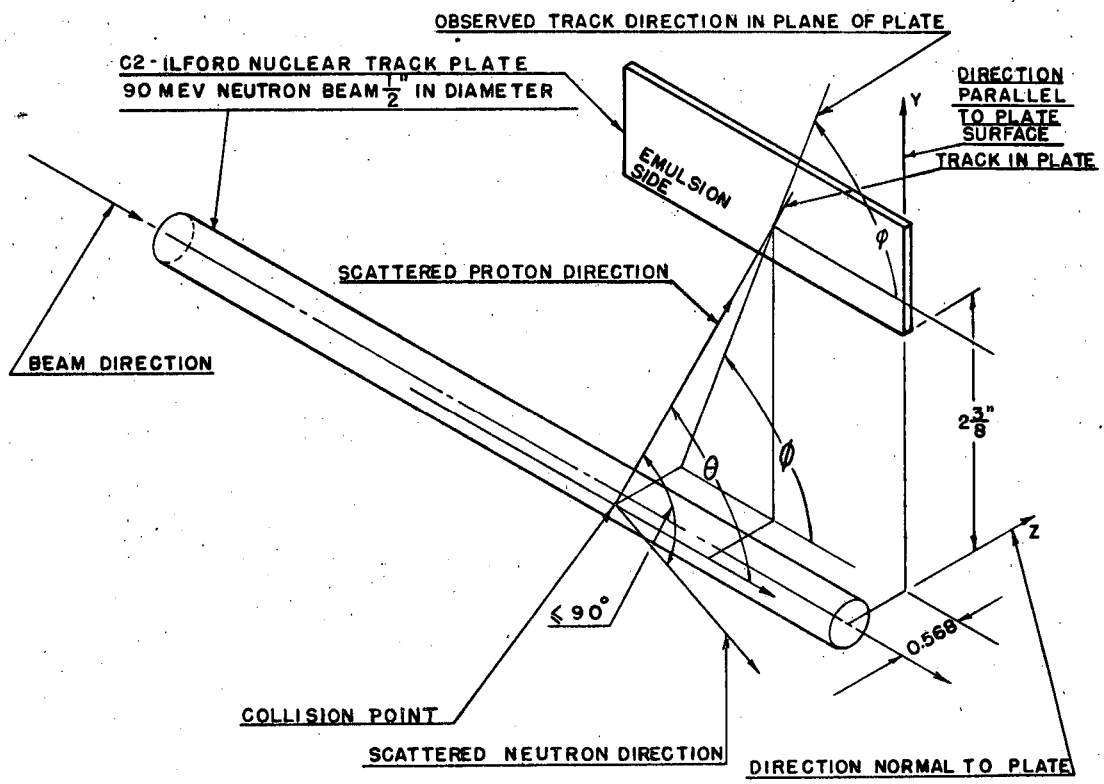
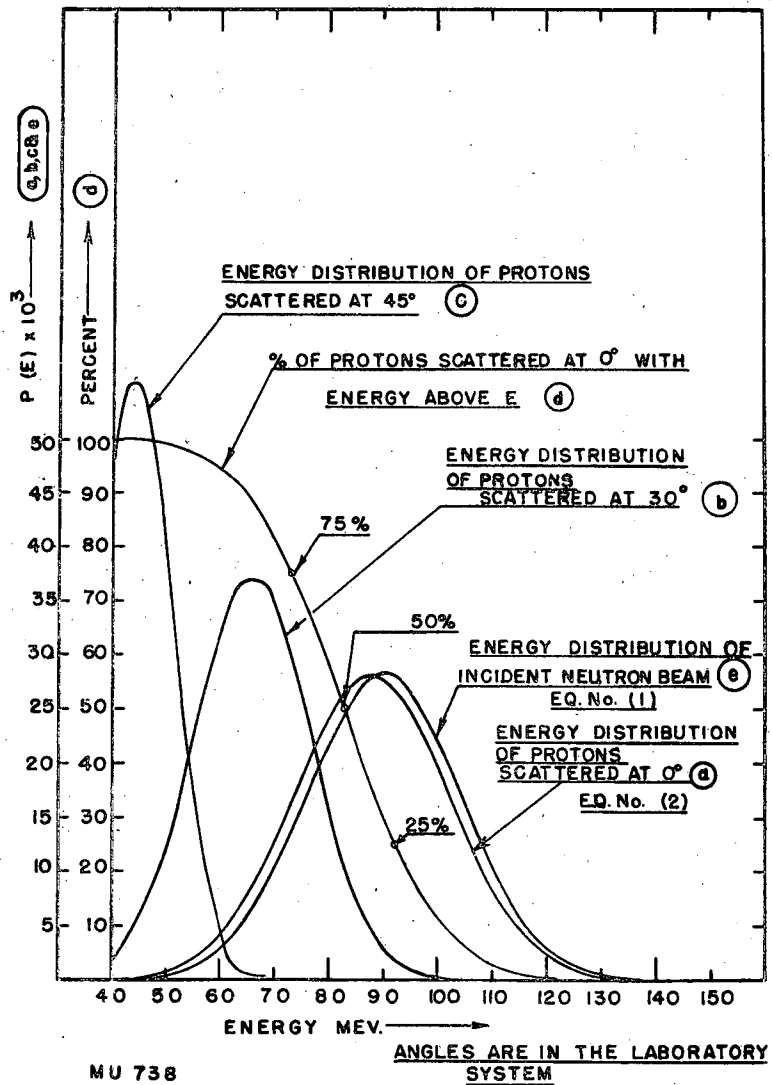


FIGURE 2

MU 737



MU 738

FIGURE 3

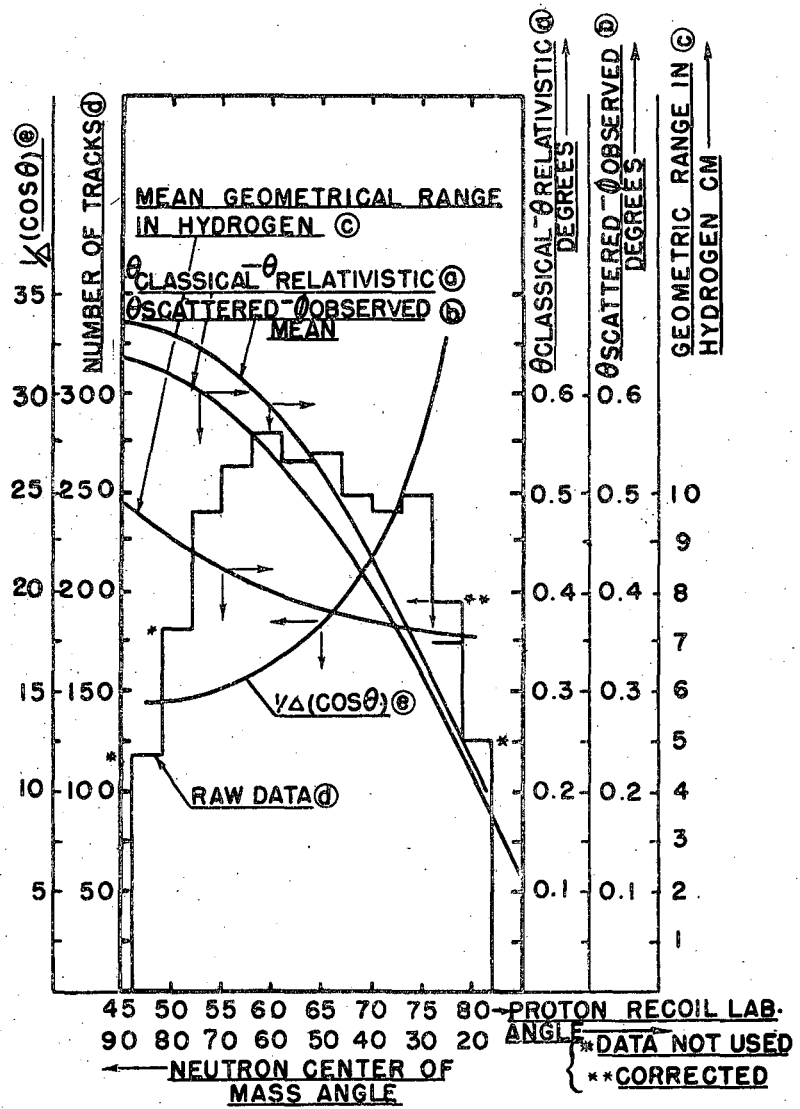
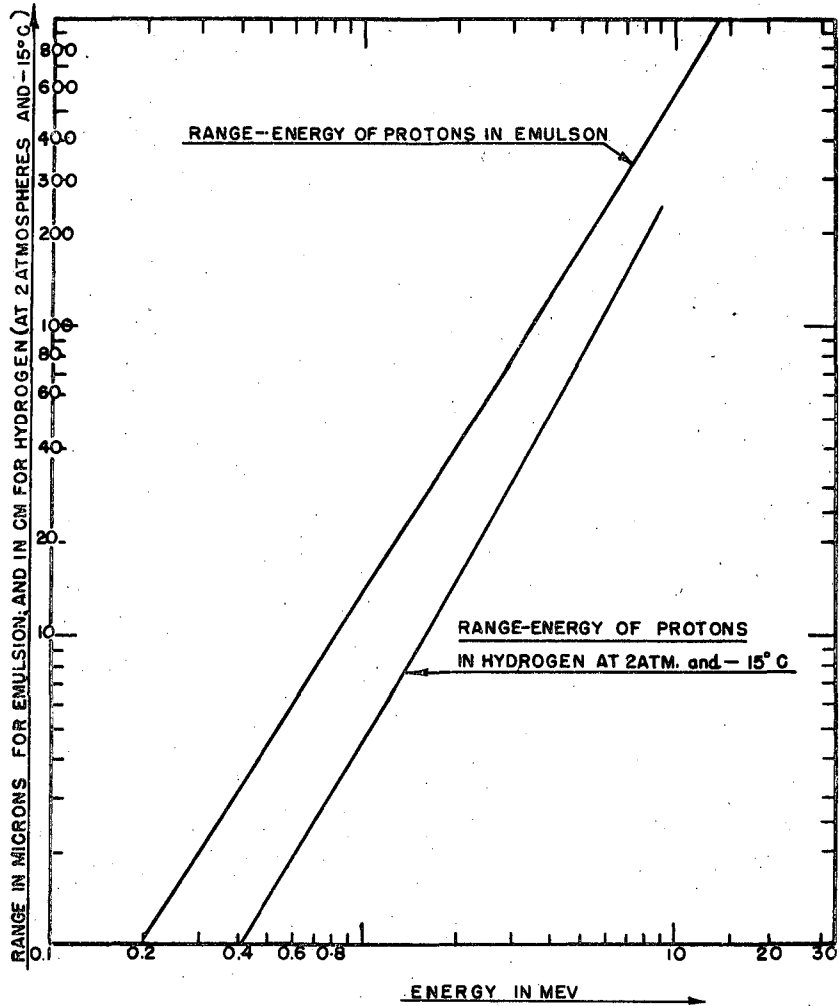


FIG. 4

MU 740



MU 739

FIGURE 5

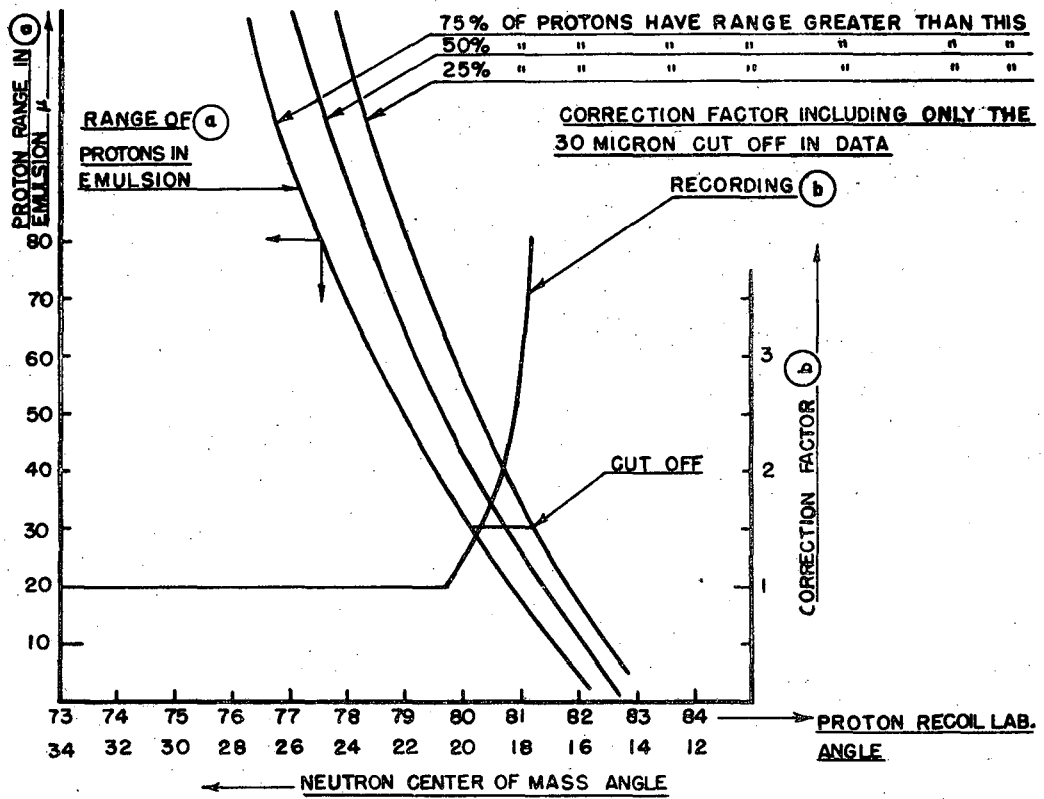


FIGURE 6

MU 741

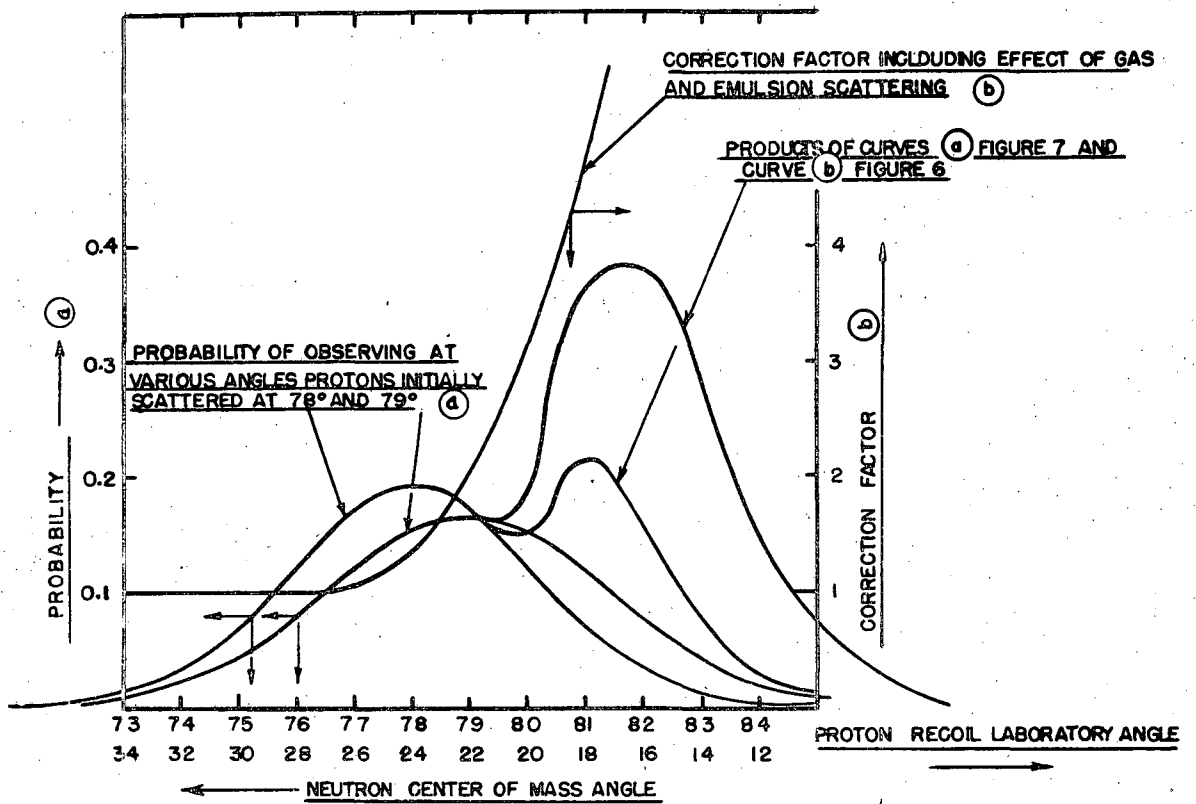


FIGURE 7

MU 742

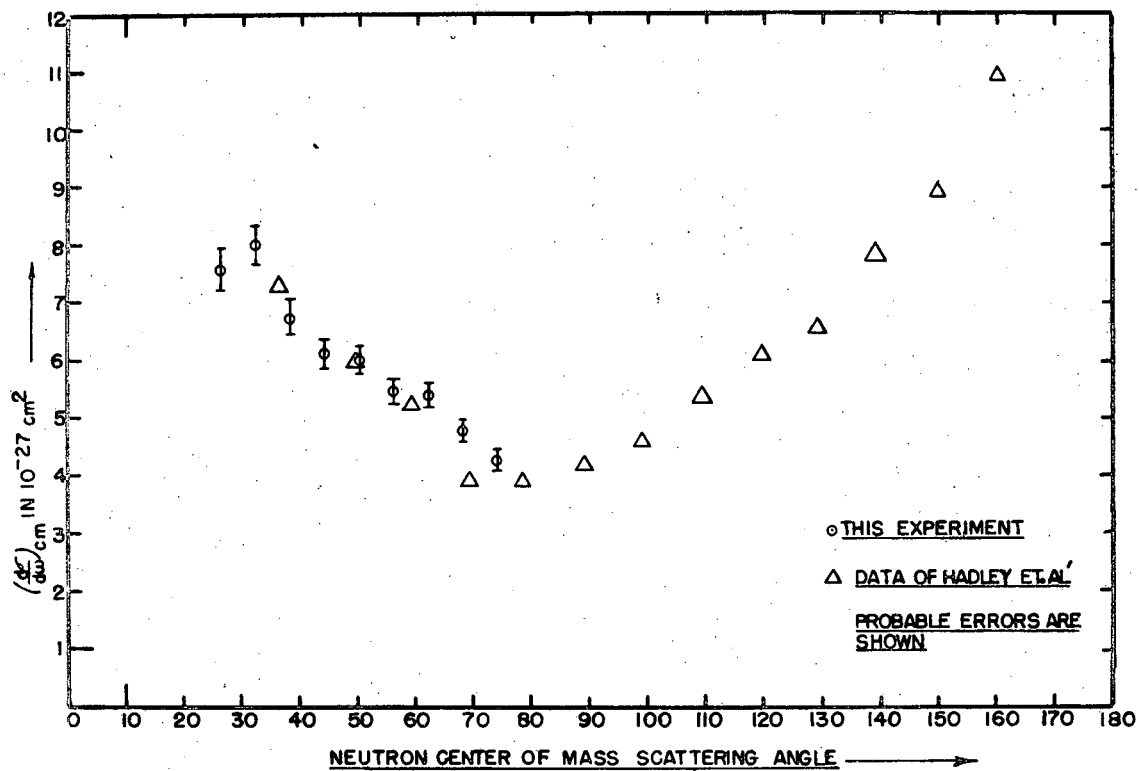


FIGURE 8

MU 743

165211